# First Observation of the $P$-Wave Spin-Singlet Bottomonium States $h_b(1P)$ and $h_b(2P)$

I. Adachi,[8] H. Aihara,[50] K. Arinstein,[1] D. M. Asner,[39] T. Aushev,[16] T. Aziz,[46] A. M. Bakich,[45] E. Barberio,[28] K. Belous,[14] V. Bhardwaj,[40] B. Bhuyan,[10] A. Bondar,[1] M. Bračko,[26,17] J. Brodzicka,[34] T. E. Browder,[7] P. Chang,[33] A. Chen,[31] P. Chen,[33] B. G. Cheon,[6] K. Chilikin,[16] R. Chistov,[16] I.-S. Cho,[55] K. Cho,[20] Y. Choi,[44] J. Dalseno,[27,47] M. Danilov,[16] Z. Drásal,[2] A. Drutskoy,[16] S. Eidelman,[1] D. Epifanov,[1] S. Esen,[3] J. E. Fast,[39] M. Feindt,[19] V. Gaur,[46] N. Gabyshev,[1] A. Garmash,[1] Y. M. Goh,[6] B. Golob,[24,17] T. Hara,[8] K. Hayasaka,[29] H. Hayashii,[30] Y. Hoshi,[48] W.-S. Hou,[33] Y. B. Hsiung,[33] H. J. Hyun,[22] T. Iijima,[29] A. Ishikawa,[49] M. Iwabuchi,[55] Y. Iwasaki,[8] I. Jaegle,[7] T. Julius,[28] J. H. Kang,[55] N. Katayama,[8] T. Kawasaki,[36] H. Kichimi,[8] H. O. Kim,[22] J. B. Kim,[21] K. T. Kim,[21] M. J. Kim,[22] Y. J. Kim,[20] K. Kinoshita,[3] B. R. Ko,[21] N. Kobayashi,[41,51] S. Koblitz,[27] S. Korpar,[26,17] P. Križan,[24,17] T. Kuhr,[19] T. Kumita,[52] A. Kuzmin,[1] Y.-J. Kwon,[55] J. S. Lange,[4] S.-H. Lee,[21] J. Li,[43] J. Libby,[11] C. Liu,[42] D. Liventsev,[16] R. Louvot,[23] J. MacNaughton,[8] D. Matvienko,[1] S. McOnie,[45] K. Miyabayashi,[30] H. Miyata,[36] Y. Miyazaki,[29] R. Mizuk,[16] G. B. Mohanty,[46] R. Mussa,[15] Y. Nagasaka,[9] E. Nakano,[38] M. Nakao,[8] H. Nakazawa,[31] Z. Natkaniec,[34] S. Neubauer,[19] S. Nishida,[8] K. Nishimura,[7] O. Nitoh,[53] T. Nozaki,[8] T. Ohshima,[29] S. Okuno,[18] S. L. Olsen,[43,7] Y. Onuki,[49] P. Pakhlov,[16] G. Pakhlova,[16] H. Park,[22] T. K. Pedlar,[25] R. Pestotnik,[17] M. Petrič,[17] L. E. Piilonen,[54] A. Poluektov,[1] M. Ritter,[27] M. Röhrken,[19] S. Ryu,[43] H. Sahoo,[7] Y. Sakai,[8] T. Sanuki,[49] O. Schneider,[23] C. Schwanda,[13] A. J. Schwartz,[3] K. Senyo,[29] O. Seon,[29] M. E. Sevior,[28] M. Shapkin,[14] V. Shebalin,[1] T.-A. Shibata,[41,51] J.-G. Shiu,[33] B. Shwartz,[1] F. Simon,[27,47] P. Smerkol,[17] Y.-S. Sohn,[55] A. Sokolov,[14] E. Solovieva,[16] S. Stanič,[37] M. Starič,[17] M. Sumihama,[41,5] G. Tatishvili,[39] Y. Teramoto,[38] I. Tikhomirov,[16] K. Trabelsi,[8] M. Uchida,[41,51] S. Uehara,[8] T. Uglov,[16] Y. Unno,[6] S. Uno,[8] S. E. Vahsen,[7] G. Varner,[7] K. E. Varvell,[45] A. Vinokurova,[1] C. H. Wang,[32] X. L. Wang,[12] Y. Watanabe,[18] J. Wicht,[8] E. Won,[21] B. D. Yabsley,[45] Y. Yamashita,[35] C. Z. Yuan,[12] V. Zhilich,[1] and A. Zupanc[19]

(Belle Collaboration)

[1]*Budker Institute of Nuclear Physics SB RAS and Novosibirsk State University, Novosibirsk 630090*
[2]*Faculty of Mathematics and Physics, Charles University, Prague*
[3]*University of Cincinnati, Cincinnati, Ohio 45221*
[4]*Justus-Liebig-Universität Gießen, Gießen*
[5]*Gifu University, Gifu*
[6]*Hanyang University, Seoul*
[7]*University of Hawaii, Honolulu, Hawaii 96822*
[8]*High Energy Accelerator Research Organization (KEK), Tsukuba*
[9]*Hiroshima Institute of Technology, Hiroshima*
[10]*Indian Institute of Technology Guwahati, Guwahati*
[11]*Indian Institute of Technology Madras, Madras*
[12]*Institute of High Energy Physics, Chinese Academy of Sciences, Beijing*
[13]*Institute of High Energy Physics, Vienna*
[14]*Institute of High Energy Physics, Protvino*
[15]*INFN - Sezione di Torino, Torino*
[16]*Institute for Theoretical and Experimental Physics, Moscow*
[17]*J. Stefan Institute, Ljubljana*
[18]*Kanagawa University, Yokohama*
[19]*Institut für Experimentelle Kernphysik, Karlsruher Institut für Technologie, Karlsruhe*
[20]*Korea Institute of Science and Technology Information, Daejeon*
[21]*Korea University, Seoul*
[22]*Kyungpook National University, Taegu*
[23]*École Polytechnique Fédérale de Lausanne (EPFL), Lausanne*
[24]*Faculty of Mathematics and Physics, University of Ljubljana, Ljubljana*
[25]*Luther College, Decorah, Iowa 52101*
[26]*University of Maribor, Maribor*
[27]*Max-Planck-Institut für Physik, München*
[28]*University of Melbourne, School of Physics, Victoria 3010*
[29]*Nagoya University, Nagoya*
[30]*Nara Women's University, Nara*
[31]*National Central University, Chung-li*

 

[32]National United University, Miao Li
[33]Department of Physics, National Taiwan University, Taipei
[34]H. Niewodniczanski Institute of Nuclear Physics, Krakow
[35]Nippon Dental University, Niigata
[36]Niigata University, Niigata
[37]University of Nova Gorica, Nova Gorica
[38]Osaka City University, Osaka
[39]Pacific Northwest National Laboratory, Richland, Washington 99352
[40]Panjab University, Chandigarh
[41]Research Center for Nuclear Physics, Osaka
[42]University of Science and Technology of China, Hefei
[43]Seoul National University, Seoul
[44]Sungkyunkwan University, Suwon
[45]School of Physics, University of Sydney, NSW 2006
[46]Tata Institute of Fundamental Research, Mumbai
[47]Excellence Cluster Universe, Technische Universität München, Garching
[48]Tohoku Gakuin University, Tagajo
[49]Tohoku University, Sendai
[50]Department of Physics, University of Tokyo, Tokyo
[51]Tokyo Institute of Technology, Tokyo
[52]Tokyo Metropolitan University, Tokyo
[53]Tokyo University of Agriculture and Technology, Tokyo
[54]CNP, Virginia Polytechnic Institute and State University, Blacksburg, Virginia 24061
[55]Yonsei University, Seoul

(Received 2 August 2011; published 18 January 2012)

We report the first observations of the spin-singlet bottomonium states $h_b(1P)$ and $h_b(2P)$. The states are produced in the reaction $e^+e^- \to h_b(nP)\pi^+\pi^-$ using a 121.4 fb$^{-1}$ data sample collected at energies near the $\Upsilon(5S)$ resonance with the Belle detector at the KEKB asymmetric-energy $e^+e^-$ collider. We determine $M[h_b(1P)] = (9898.2^{+1.1+1.0}_{-1.0-1.1})$ MeV/$c^2$ and $M[h_b(2P)] = (10\,259.8 \pm 0.6^{+1.4}_{-1.0})$ MeV/$c^2$, which correspond to $P$-wave hyperfine splittings $\Delta M_{\rm HF} = (+1.7 \pm 1.5)$ and $(+0.5^{+1.6}_{-1.2})$ MeV/$c^2$, respectively. The significances of the $h_b(1P)$ and $h_b(2P)$ are $5.5\sigma$ and $11.2\sigma$, respectively. We find that the production of the $h_b(1P)$ and $h_b(2P)$ is not suppressed relative to the production of the $\Upsilon(1S)$, $\Upsilon(2S)$, and $\Upsilon(3S)$.

DOI: 10.1103/PhysRevLett.108.032001 PACS numbers: 13.25.Gv, 14.40.Pq, 12.39.Pn

Bottomonium is the bound system of $b\bar{b}$ quarks and is considered an excellent laboratory to study quantum chromodynamics (QCD) at low energies. The system is approximately nonrelativistic due to the large $b$-quark mass, and therefore the quark-antiquark QCD potential can be investigated via $b\bar{b}$ spectroscopy [1].

The spin-singlet states $h_b(nP)$ and $\eta_b(nS)$ alone provide information concerning the spin-spin (or hyperfine) interaction in bottomonium. Measurements of the $h_b(nP)$ masses provide unique access to the $P$-wave hyperfine splitting $\Delta M_{\rm HF} \equiv \langle M(n^3P_J)\rangle - M(n^1P_1)$, the difference between the spin-weighted average mass of the $P$-wave triplet states [$\chi_{bJ}(nP)$ or $n^3P_J$] and that of the corresponding $h_b(nP)$, or $n^1P_1$. The hyperfine splitting for the $1P$ charmonium states has been measured recently to be very small: $\Delta M_{\rm HF} = (0.00 \pm 0.15)$ MeV/$c^2$ [2]. The hyperfine splitting in bottomonium is expected to be smaller than in charmonium due to its higher mass [3].

Recently, the CLEO Collaboration observed the process $e^+e^- \to h_c(1P)\pi^+\pi^-$ at a rate comparable to that for $e^+e^- \to J/\psi\pi^+\pi^-$ in data taken above the open charm threshold [4]. Such a large rate was unexpected because the production of $h_c(1P)$ requires a $c$-quark spin flip, while production of $J/\psi$ does not. Similarly, the Belle Collaboration observed anomalously high rates for $e^+e^- \to \Upsilon(nS)\pi^+\pi^-$ $(n = 1, 2, 3)$ at energies near the $\Upsilon(5S)$ mass [5]. Together, these observations motivate a search for $e^+e^- \to \pi^+\pi^- h_b(nP)$ above the open-bottom threshold at the $\Upsilon(5S)$ resonance.

In this Letter, we report the first observation of the $h_b(1P)$ and $h_b(2P)$ produced via $e^+e^- \to h_b(nP)\pi^+\pi^-$ in the $\Upsilon(5S)$ region. We use a 121.4 fb$^{-1}$ data sample collected near the peak of the $\Upsilon(5S)$ resonance ($\sqrt{s} \sim 10.865$ GeV) with the Belle detector [6] at the KEKB asymmetric-energy $e^+e^-$ collider [7].

We observe the $h_b(nP)$ states in the $\pi^+\pi^-$ missing mass spectrum of hadronic events. The $\pi^+\pi^-$ missing mass is defined as $M^2_{\rm miss} \equiv (P_{\Upsilon(5S)} - P_{\pi^+\pi^-})^2$, where $P_{\Upsilon(5S)}$ is the 4-momentum of the $\Upsilon(5S)$ determined from the beam momenta and $P_{\pi^+\pi^-}$ is the 4-momentum of the $\pi^+\pi^-$ system.

The $\pi^+\pi^-$ transitions between $\Upsilon(nS)$ states provide high-statistics reference signals. A high purity sample

of such transitions is obtained by reconstructing $\mu^+\mu^-\pi^+\pi^-$ combinations. We select tracks that originate from the vicinity of the run-averaged interaction point. The pion candidates are identified based on the ionization energy loss measurement in the central drift chamber and the response of the aerogel Cherenkov counters and time-of-flight system. In addition, electromagnetic calorimeter information is used to veto electrons. Muons are identified by their range and transverse scattering in the instrumented flux return of the Belle solenoid. To suppress the process $e^+e^- \to \mu^+\mu^-\gamma(\to e^+e^-)$, where the conversion $e^+e^-$ pair is misidentified as $\pi^+\pi^-$, we require that the opening angle between the candidate pions in the laboratory frame satisfies $\cos\theta_{\pi^+\pi^-} < 0.95$. In Fig. 1(a), we present the two-dimensional distribution of $\mu^+\mu^-$ mass $M_{\mu^+\mu^-}$ vs $M_{\rm miss}$ for events satisfying these criteria.

Clear clusters are visible along a diagonal band, where $M_{\mu^+\mu^-}$ is roughly equal to $M_{\rm miss}$, and correspond to fully reconstructed $\Upsilon(5S) \to \Upsilon(nS)\pi^+\pi^- \to \mu^+\mu^-\pi^+\pi^-$ events. The band along the diagonal is due to the remaining $e^+e^- \to \mu^+\mu^-\gamma(\to e^+e^-)$ background or due to the non-resonant $e^+e^- \to \mu^+\mu^-\pi^+\pi^-$ process. Events along the diagonal satisfying $|M_{\rm miss} - M_{\mu^+\mu^-}| < 150$ MeV$/c^2$ are projected onto the $M_{\rm miss}$ axis and fitted to the sum of a linear background and a Gaussian joined to a power-law tail on the high mass side. The natural widths of the $\Upsilon(nS)$ states are negligible compared to the detector resolution. The high-side tail is due to initial state radiation photons. This latter function is analogous to the well-known Crystal Ball function [8] but has the tail on the higher rather than the lower side. We thus refer to it as a "reversed Crystal Ball" (rCB) function. The fitted $M_{\rm miss}$ spectra from this band are shown in Figs. 1(b)–1(d), and the resulting yields, deviations of peak positions from world average values [9], and width parameters ($\sigma$) of the rCB function for the $\Upsilon(nS)$ states are displayed in Table I. The masses obtained are consistent with the world average values.

The structures in the horizontal band in Fig. 1(a), where $M_{\mu^+\mu^-}$ is roughly equal to $M[\Upsilon(1S)]$, arise from events in which a daughter $\Upsilon(1S)$ in the event decays to $\mu^+\mu^-$. In Figs. 1(e) and 1(f), we present $M_{\rm miss}$ projections from this band, subject to the requirement $|M_{\mu^+\mu^-} - M[\Upsilon(1S)]| < 150$ MeV$/c^2$. The peaks at the $\Upsilon(3S)$ and $\Upsilon(2S)$ masses arise from events having $\pi^+\pi^-$ transitions to $\Upsilon(3S)$ or $\Upsilon(2S)$, followed by inclusive production of $\Upsilon(1S)$, and are fitted to rCB functions. Peaks at 9.97 and 10.30 GeV$/c^2$ arise from events in which a $\Upsilon(3S)$ or $\Upsilon(2S)$ is produced inclusively in $\Upsilon(5S)$ decays or via initial state radiation, and then decays to $\Upsilon(1S)\pi^+\pi^-$, and are fitted to single and double Gaussians, respectively.

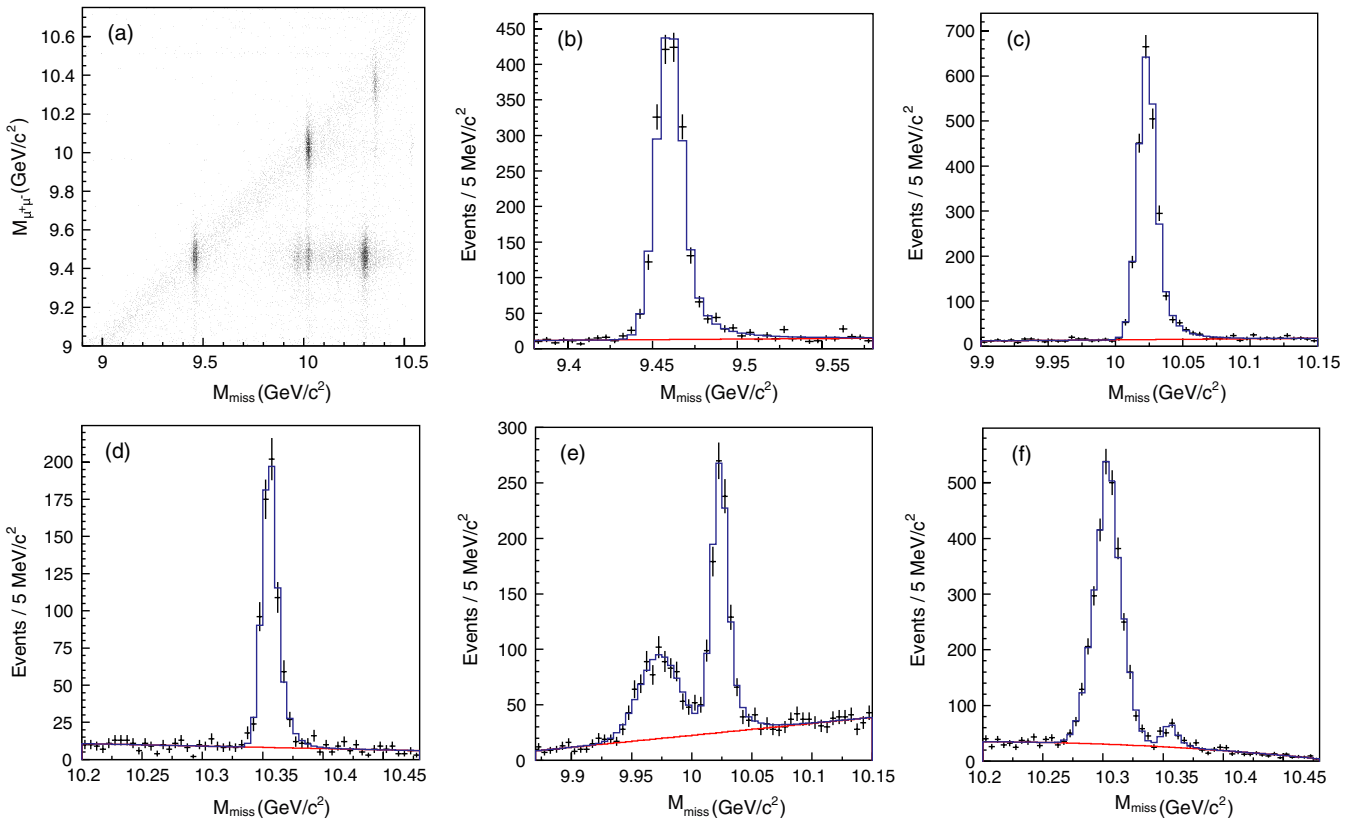


FIG. 1 (color online). (a) Distribution of $M_{\mu^+\mu^-}$ vs $M_{\rm miss}$, and the projection on $M_{\rm miss}$ from (b)–(d), the diagonal band $|M_{\rm miss} - M_{\mu^+\mu^-}| < 150$ MeV$/c^2$ near the $\Upsilon(1S)$, $\Upsilon(2S)$, and $\Upsilon(3S)$; and (e),(f) the horizontal band $|M_{\mu^+\mu^-} - M[\Upsilon(1S)]| < 150$ MeV$/c^2$ near the $\Upsilon(2S)$ and $\Upsilon(3S)$.

TABLE I. The yield, deviation of peak position from world average value, and width ($\sigma$) for signals reconstructed by using $M_{\rm miss}$ from the exclusive $\mu^+\mu^-\pi^+\pi^-$ selection. For mass differences the first error is statistical, and the second one is the error in the world average value [9].

| | Yield | Mass, MeV/$c^2$ | $\sigma$, MeV/$c^2$ |
|---|---|---|---|
| $\Upsilon(1S)$ | $1894 \pm 61$ | $-0.34 \pm 0.23 \pm 0.26$ | $7.68 \pm 0.21$ |
| $\Upsilon(2S)$ | $2322 \pm 60$ | $+0.08 \pm 0.22 \pm 0.31$ | $6.60 \pm 0.20$ |
| $\Upsilon(3S)$ | $661^{+39}_{-30}$ | $+0.42^{+0.56}_{-0.39} \pm 0.5$ | $5.98^{+0.62}_{-0.37}$ |

To reconstruct the $\Upsilon(5S) \to h_b(nP)\pi^+\pi^-$ transitions inclusively, we use a general hadronic event selection with requirements on the position of the primary vertex, track multiplicity, and total energy and momentum of the event [10]. These requirements suppress $\tau^+\tau^-$, quantum electrodynamic, two-photon, and beam gas processes but are very efficient for the bottomonium decays to hadrons. The background from continuum $e^+e^- \to q\bar{q}$ ($q = u, d, s, c$) processes has a jetlike shape as opposed to the spherically symmetric signal events and is suppressed by requiring the ratio of the second to zeroth Fox-Wolfram moments to satisfy $R_2 < 0.3$ [11]. The selection of the $\pi^+\pi^-$ candidates is the same as described above for the $\mu^+\mu^-\pi^+\pi^-$ sample except that no requirement on the opening angle is applied. These selection requirements are optimized by maximizing the significance of the high-statistics reference channel $\Upsilon(5S) \to \Upsilon(2S)\pi^+\pi^-$ (extraction of this signal is described below). The resulting $M_{\rm miss}$ spectrum, which is dominated by combinatoric $\pi^+\pi^-$ pairs, is shown in Fig. 2. The typical momenta of signal pions in the center-of-mass frame range from 170 to 700 MeV/$c$.

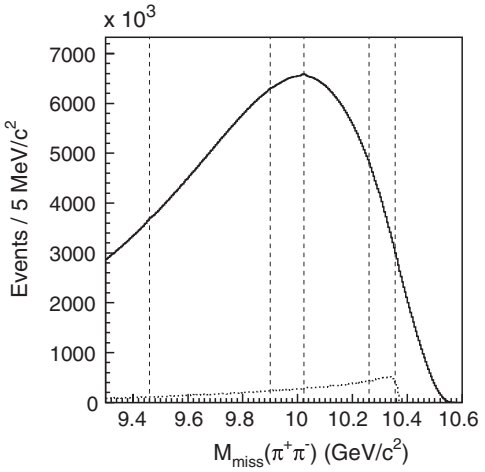


FIG. 2. The $M_{\rm miss}$ distribution for the selected $\pi^+\pi^-$ pairs (solid histogram) and $K^0_S \to \pi^+\pi^-$ reflection multiplied by a factor 10 to make it visible (dotted histogram). Vertical lines indicate the locations of the $\Upsilon(1S)$, $h_b(1P)$, $\Upsilon(2S)$, $h_b(2P)$, and $\Upsilon(3S)$ signals.

The threshold for inclusive $K^0_S$ production results in a sharp rise in the $M_{\rm miss}$ spectrum, due to $K^0_S \to \pi^+\pi^-$, very close to the mass of $\Upsilon(3S)$ (see Fig. 2). Rather than veto $\pi^+\pi^-$ combinations with invariant masses near $M(K^0_S)$, which significantly distorts the $M_{\rm miss}$ spectrum in the vicinity, we obtain the $K^0_S$ contamination by fitting the $\pi^+\pi^-$ invariant mass corresponding to bins of $M_{\rm miss}$.

The $M_{\rm miss}$ spectrum is divided into three adjacent regions with boundaries at $M_{\rm miss} = 9.3$, 9.8, 10.1, and 10.45 GeV/$c^2$ and fitted separately in each region. In the third region, prior to fitting, we subtract the contribution due to $K^0_S \to \pi^+\pi^-$ bin by bin. The signal component of the fit includes all signals seen in the $\mu^+\mu^-\pi^+\pi^-$ data as well as those arising from $\pi^+\pi^-$ transitions to $h_b(nP)$ and $\Upsilon(1D)$. Monte Carlo studies indicate that the shape of the peaks in $M_{\rm miss}$ is independent of whether the $\pi^+\pi^-$ are reconstructed in the hadronic environment or in the much cleaner environment of exclusively reconstructed $\mu^+\mu^-\pi^+\pi^-$ events. Therefore, in the inclusive analysis we use shapes determined from the $\mu^+\mu^-\pi^+\pi^-$ sample. For the additional $h_b(nP)$ and $\Upsilon(1D)$ signals, we use the tail parameters of the $\Upsilon(2S)$ and the width parameters ($\sigma$) found by linear interpolation in mass from the widths of the exclusively reconstructed $\Upsilon(nS)$ peaks. The peak positions of all signals are floated, except that for $\Upsilon(3S) \to \Upsilon(1S)\pi^+\pi^-$, which is poorly constrained by the fit. In the first two regions, the combinatorial background is described by a 6th-order Chebyshev polynomial, while in the third we use a 7th-order one. We perform binned $\chi^2$ fits to each region using 1 MeV/$c^2$ bins, though for clarity we display the data in 5 MeV/$c^2$ bins. The confidence levels of the fits in the three regions are 78%, 80%, and 30%, respectively. The $M_{\rm miss}$ spectrum after subtraction of both the combinatoric and $K^0_S \to \pi^+\pi^-$ contributions is shown with the fitted signal functions overlaid in Fig. 3. The signal parameters are listed in Table II.

We studied several sources of systematic uncertainty. The background polynomial order was increased by three, and the range of the fits performed were altered by up to 100 MeV/$c^2$. Different signal functions were used, including symmetric Gaussians and rCB functions with the width parameters left free. We altered our selection criteria: tightening the requirements on the proximity of track origin to the IP, requiring at least five tracks in the event, and imposing the $\cos\theta_{\pi^+\pi^-} < 0.95$ requirement used in the $\mu^+\mu^-\pi^+\pi^-$ study. In Table III, the results of these systematic studies are summarized.

The values in the table represent the maximal change of parameters under the variations explored. We estimate an additional 1 MeV/$c^2$ uncertainty in mass measurements based on the differences between the observed values of the fitted $\Upsilon(nS)$ peak positions and their world averages. These deviations could be due to the local variations of the background shape that are not adequately described by the polynomial. The total systematic uncertainties presented in

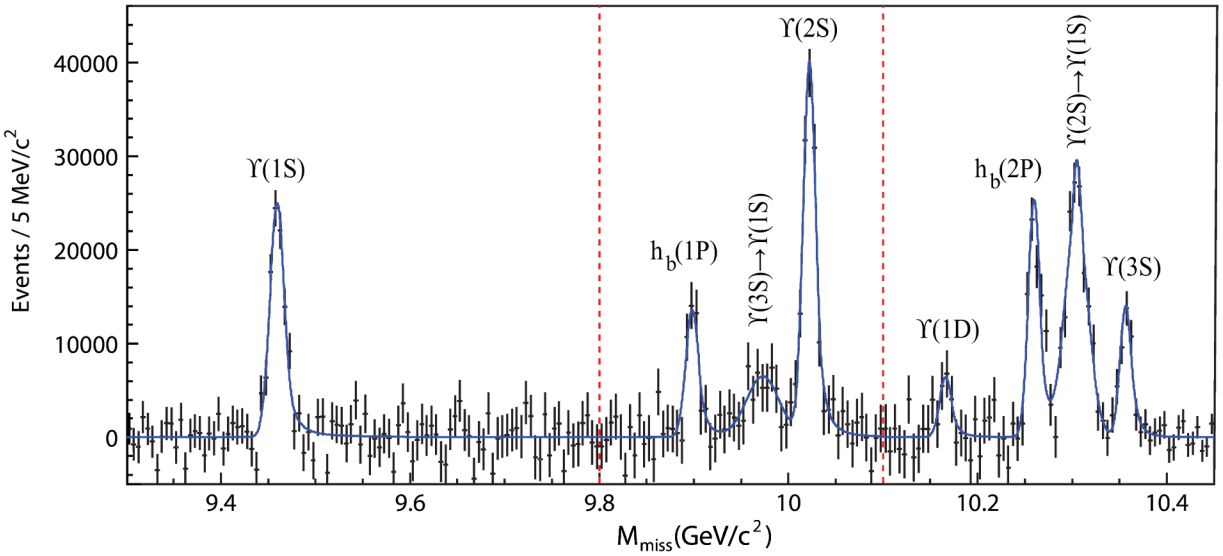


FIG. 3 (color online). The inclusive $M_{\rm miss}$ spectrum with the combinatoric background and $K^0_S$ contribution subtracted (points with errors) and signal component of the fit function overlaid (smooth curve). The vertical lines indicate boundaries of the fit regions.

Table II represent the sum in quadrature of all the contributions listed in Table III. The signal for the $\Upsilon(1D)$ is marginal, and therefore systematic uncertainties on its related measurements are not listed in the table. The significances of the $h_b(1P)$ and $h_b(2P)$ signals, with systematic uncertainties accounted for, are $5.5\sigma$ and $11.2\sigma$, respectively.

The measured masses of $h_b(1P)$ and $h_b(2P)$ are $M = (9898.2^{+1.1+1.0}_{-1.0-1.1})$ MeV/$c^2$ and $M = (10259.8 \pm 0.6^{+1.4}_{-1.0})$ MeV/$c^2$, respectively. Using the world average masses of the $\chi_{bJ}(nP)$ states, we determine the hyperfine splittings to be $\Delta M_{\rm HF} = (+1.7 \pm 1.5)$ and $(+0.5^{+1.6}_{-1.2})$ MeV/$c^2$, respectively, where statistical and systematic uncertainties are combined in quadrature.

We also measure the ratio of cross sections for $e^+e^- \to \Upsilon(5S) \to h_b(nP)\pi^+\pi^-$ to that for $e^+e^- \to \Upsilon(5S) \to \Upsilon(2S)\pi^+\pi^-$. To determine the reconstruction efficiency, we use the results of resonant structure studies reported in Ref. [12] that revealed the existence of two charged bottomoniumlike states, $Z_b(10610)$ and $Z_b(10650)$, through which the $\pi^+\pi^-$ transitions we are studying primarily proceed. These studies indicate that the $Z_b$ most likely have $J^P = 1^+$, and therefore in our simulations the $\pi^+\pi^-$ transitions are generated accordingly. To estimate the systematic uncertainty in our reconstruction efficiencies, we use Monte Carlo samples generated with all allowed quantum numbers with $J \leq 2$.

We find that the reconstruction efficiency for the $\Upsilon(2S)$ is about 57% and that those for the $h_b(1P)$ and $h_b(2P)$ relative to that for the $\Upsilon(2S)$ are $0.913^{+0.136}_{-0.010}$ and $0.824^{+0.130}_{-0.013}$, respectively. The efficiency of the $R_2 < 0.3$ requirement is estimated from data by measuring signal yields with $R_2 > 0.3$. For $\Upsilon(2S)$, $h_b(1P)$, and $h_b(2P)$ we find $0.863 \pm 0.032$, $0.723 \pm 0.068$, and $0.796 \pm 0.043$, respectively. From the yields and efficiencies

TABLE II. The yield, mass, and statistical significance from the fits to the $M_{\rm miss}$ distributions. The statistical significance is calculated from the difference in $\chi^2$ between the best fit and the fit with the signal yield fixed to zero.

| | Yield, $10^3$ | Mass, MeV/$c^2$ | Significance |
|---|---|---|---|
| $\Upsilon(1S)$ | $104.9 \pm 5.8 \pm 3.0$ | $9459.4 \pm 0.5 \pm 1.0$ | $18.1\sigma$ |
| $h_b(1P)$ | $50.0 \pm 7.8^{+4.5}_{-9.1}$ | $9898.2^{+1.1+1.0}_{-1.0-1.1}$ | $6.1\sigma$ |
| $3S \to 1S$ | $55 \pm 19$ | 9973.01 | $2.9\sigma$ |
| $\Upsilon(2S)$ | $143.7 \pm 8.7 \pm 6.8$ | $10\,022.2 \pm 0.4 \pm 1.0$ | $17.1\sigma$ |
| $\Upsilon(1D)$ | $22.4 \pm 7.8$ | $10\,166.1 \pm 2.6$ | $2.4\sigma$ |
| $h_b(2P)$ | $83.9 \pm 6.8^{+23.}_{-10.}$ | $10\,259.8 \pm 0.6^{+1.4}_{-1.0}$ | $12.3\sigma$ |
| $2S \to 1S$ | $151.3 \pm 9.7^{+9.0}_{-20.}$ | $10\,304.6 \pm 0.6 \pm 1.0$ | $15.7\sigma$ |
| $\Upsilon(3S)$ | $45.5 \pm 5.2 \pm 5.1$ | $10\,356.7 \pm 0.9 \pm 1.1$ | $8.5\sigma$ |

TABLE III. Absolute systematic uncertainties in the yields and masses from various sources.

| | Polynomial order | Fit range | Signal shape | Selection requirements |
|---|---|---|---|---|
| $N[\Upsilon(1S)]$, $10^3$ | $\pm 1.4$ | $\pm 1.7$ | $\pm 2.0$ | $\cdots$ |
| $N[h_b(1P)]$, $10^3$ | $\pm 2.4$ | $\pm 3.6$ | $^{+1.2}_{-8.0}$ | $\cdots$ |
| $N[\Upsilon(2S)]$, $10^3$ | $\pm 3.4$ | $\pm 3.2$ | $\pm 5.0$ | $\cdots$ |
| $N[h_b(2P)]$, $10^3$ | $\pm 2.2$ | $\pm 2.6$ | $^{+23.}_{-9.0}$ | $\cdots$ |
| $N[2 \to 1]$, $10^3$ | $\pm 3.0$ | $\pm 8.0$ | $^{+0}_{-18}$ | $\cdots$ |
| $N[\Upsilon(3S)]$, $10^3$ | $\pm 1.0$ | $\pm 3.0$ | $\pm 4.0$ | $\cdots$ |
| $M[\Upsilon(1S)]$, MeV/$c^2$ | $\pm 0.04$ | $\pm 0.06$ | $\pm 0.03$ | $\pm 0.18$ |
| $M[h_b(1P)]$, MeV/$c^2$ | $\pm 0.04$ | $\pm 0.10$ | $^{+0.04}_{-0.20}$ | $^{+0.20}_{-0.30}$ |
| $M[\Upsilon(2S)]$, MeV/$c^2$ | $\pm 0.02$ | $\pm 0.08$ | $\pm 0.06$ | $\pm 0.03$ |
| $M[h_b(2P)]$, MeV/$c^2$ | $\pm 0.10$ | $\pm 0.20$ | $^{+1.0}_{-0.0}$ | $\pm 0.08$ |
| $M[2 \to 1]$, MeV/$c^2$ | $\pm 0.20$ | $\pm 0.10$ | $\pm 0.06$ | $\pm 0.10$ |
| $M[\Upsilon(3S)]$, MeV/$c^2$ | $\pm 0.15$ | $\pm 0.24$ | $\pm 0.10$ | $\pm 0.20$ |

described above, we determine the ratio of cross sections $R \equiv \frac{\sigma(h_b(nP)\pi^+\pi^-)}{\sigma(\Upsilon(2S)\pi^+\pi^-)}$ to be $R = 0.45 \pm 0.08^{+0.07}_{-0.12}$ for the $h_b(1P)$ and $R = 0.77 \pm 0.08^{+0.22}_{-0.17}$ for the $h_b(2P)$. Hence, $\Upsilon(5S) \to h_b(nP)\pi^+\pi^-$ and $\Upsilon(5S) \to \Upsilon(2S)\pi^+\pi^-$ proceed at similar rates, despite the fact that the production of $h_b(nP)$ requires a spin flip of a $b$ quark.

The rate of $\Upsilon(5S) \to h_b(nP)\pi^+\pi^-$ is much larger than the upper limit for that of $\Upsilon(3S) \to h_b(nP)\pi^+\pi^-$ obtained by the *BABAR* Collaboration [13]. This is consistent with the observation that the rates for $\Upsilon(5S) \to \Upsilon(mS)\pi^+\pi^-$ with $m = 1, 2, 3$ are much larger than those for $\Upsilon(nS) \to \Upsilon(mS)\pi^+\pi^-$ for $n = 2, 3, 4$ [5]. The only previous evidence for the $h_b(1P)$ is a $3.0\sigma$ excess in $\Upsilon(3S) \to \pi^0 h_b(1P)$ at $(9902 \pm 4)$ MeV/$c^2$ presented by *BABAR* [14].

We have also used 711 fb$^{-1}$ of $e^+e^-$ collisions at the $\Upsilon(4S)$ resonance to search for $\Upsilon(4S) \to h_b(1P)\pi^+\pi^-$ [for the transition to the $h_b(2P)$, the available phase space is very small]. The overall efficiency, assuming the $R_2$ efficiency at $\Upsilon(4S)$ to be the same as that at $\Upsilon(5S)$, is $0.94^{+0.11}_{-0.03}$ relative to that for $\Upsilon(5S) \to h_b(1P)\pi^+\pi^-$. From our observed yield of $(35 \pm 21^{+24}_{-15}) \times 10^3$, we set an upper limit on the ratio of $\sigma(e^+e^- \to h_b(1P)\pi^+\pi^-)$ at the $\Upsilon(4S)$ to that at the $\Upsilon(5S)$ of 0.27 at 90% C.L.

The only bottomonium states in the vicinity of the observed $h_b(nP)$ are the $\chi_{b1}(nP)$. However, the measured peak positions of the $h_b(nP)$ candidates differ from the corresponding $\chi_{b1}(nP)$ masses at the $3\sigma$ level. In addition, the transitions $\Upsilon(5S) \to \chi_{b1}(nP)\pi^+\pi^-$ violate isospin conservation. These indicate that the observed states are the $h_b(nP)$. Furthermore, recently Belle observed the $h_b(1P) \to \eta_b(1S)\gamma$ decay [15] and found that its branching fraction is in agreement with theoretical expectations [3]. This observation establishes that the $C$ parity of the $h_b(1P)$ candidate is odd and thus excludes its interpretation as the $\chi_{b1}(1P)$. The angular analysis of the $\Upsilon(5S) \to h_b(1P)\pi^+\pi^-$ transition [16] is consistent with the $h_b(1P)$ candidate spin parity of $J^P = 1^+$, as expected.

In summary, we have observed the $P$-wave spin-singlet bottomonium states $h_b(1P)$ and $h_b(2P)$ in the reaction $e^+e^- \to \Upsilon(5S) \to h_b(nP)\pi^+\pi^-$. The $h_b(nP)$ masses correspond to hyperfine splittings that are consistent with zero. We also have observed that the cross sections for these processes and that for $e^+e^- \to \Upsilon(5S) \to \Upsilon(2S)\pi^+\pi^-$ are of comparable magnitude, which indicates that the production of $h_b(nP)$ at the $\Upsilon(5S)$ resonance must occur via a process that mitigates the expected suppression related to heavy quark spin flip.

We thank the KEKB group for excellent operation of the accelerator, the KEK cryogenics group for efficient solenoid operations, and the KEK computer group, the NII, and PNNL/EMSL for valuable computing and SINET4 network support. We acknowledge support from MEXT, JSPS, and Nagoya's TLPRC (Japan); ARC and DIISR (Australia); NSFC (China); MSMT (Czechia); DST (India); MEST, NRF, NSDC of KISTI, and WCU (Korea); MNiSW (Poland); MES and RFAAE (Russia); ARRS (Slovenia); SNSF (Switzerland); NSC and MOE (Taiwan); and DOE and NSF (USA).

[1] N. Brambilla *et al.*, Eur. Phys. J. C **71**, 1534 (2011).
[2] S. Dobbs *et al.* (CLEO Collaboration), Phys. Rev. Lett. **101**, 182003 (2008); M. Albikim *et al.* (BES Collaboration), Phys. Rev. Lett. **104**, 132002 (2010).
[3] For a summary of predictions for the hyperfine splittings and corresponding references, see S. Godfrey and J. L. Rosner, Phys. Rev. D **66**, 014012 (2002).
[4] T. K. Pedlar *et al.* (CLEO Collaboration), Phys. Rev. Lett. **107**, 041803 (2011).
[5] K.-F. Chen *et al.* (Belle Collaboration), Phys. Rev. Lett. **100**, 112001 (2008).
[6] A. Abashian *et al.* (Belle Collaboration), Nucl. Instrum. Methods Phys. Res., Sect. A **479**, 117 (2002).
[7] S. Kurokawa and E. Kikutani, Nucl. Instrum. Methods Phys. Res., Sect. A **499**, 1 (2003), and other papers included in this volume.
[8] J. E. Gaiser, Ph.D. thesis, Stanford University [Report No. SLAC-R-255, 1982 (unpublished)]; T. Skwarnicki, Ph.D. thesis, Institute of Nuclear Physics, Krakow, Poland [Report No. DESY F31-86-02, 1986 (unpublished)].
[9] K. Nakamura *et al.* (Particle Data Group), J. Phys. G **37**, 075021 (2010).
[10] K. Abe *et al.* (Belle Collaboration), Phys. Rev. D **64**, 072001 (2001).
[11] G. C. Fox and S. Wolfram, Phys. Rev. Lett. **41**, 1581 (1978).
[12] A. Bondar *et al.* (Belle Collaboration), arXiv:1110.2251.
[13] J. P. Lees *et al.* (*BABAR* Collaboration), Phys. Rev. D **84**, 011104 (2011).
[14] J. P. Lees *et al.* (*BABAR* Collaboration), arXiv:1102.4565.
[15] I. Adachi *et al.* (Belle Collaboration), arXiv:1110.3934.
[16] I. Adachi *et al.* (Belle Collaboration), arXiv:1105.4583.